Title:

The peach RGF/GLV signalling peptide pCTG134 is involved in a regulatory circuit that sustains auxin and ethylene actions

Running title:

A peach peptide hormone involved in auxin-ethylene crosstalk

Nicola Busatto[1], Umberto Salvagnin[1], Francesca Resentini[1], Silvia Quaresimin[1], Lorella Navazio[1], Oriano Marin[2], Maria Pellegrini[3], Fabrizio Costa[4], Dale F. Mierke[3], Livio Trainotti[1]

Highlight:

The role of the peach RGF/GLV peptide during root hair formation in *Arabidopsis* and tobacco supports its involvement in a cross-hormonal auxin-ethylene regulatory circuit.

[1] *Department of Biology, University of Padova, Viale G. Colombo 3, I-35131 Padova, Italy*

[2] *Department of Biomedical Sciences, University of Padova, Viale G. Colombo 3, I-35131 Padova, Italy*

[3] *Chemistry Department, Dartmouth College, 03755 Hanover, NH, United States of America*

[4] *Research and Innovation Centre, Fondazione Edmund Mach, Via Mach 1, 38010 San Michele all'Adige, Trento, Italy*

Email addresses

Nicola Busatto: nicola.busatto@fmach.it

Umberto Salvagnin: umberto.salvagnin@unipd.it

Francesca Resentini: francesca.resentini@gmail.com

Silvia Quaresimin: silvia.quaresimin@unipd.it

Lorella Navazio: lorella.navazio@unipd.it

Oriano Marin: oriano.marin@unipd.it

Maria Pellegrini: Maria.Pellegrini@dartmouth.edu

Fabrizio Costa: fabrizio.costa@fmach.it
Dale F. Mierke: Dale.F.Mierke@dartmouth.edu
Livio Trainotti: telephone: +39 049 8276292; email: livio.trainotti@unipd.it

Date of submission: May 24th 2017
Total word count: 5575
No. of tables : 0
No. of figures: 9
Fig. 1 online: colour; printed: black and white
Fig. 2 online: colour; printed: colour
Fig. 3 online: colour; printed: colour
Fig. 4 online: colour; printed: black and white
Fig. 5 online: black and white; printed: black and white
Fig. 6 online: colour; printed: black and white
Fig. 7 online: black and white; printed: black and white
Fig. 8 online: black and white; printed: black and white
Fig. 9 online: colour; printed: black and white
Supplementary tables: 1
Supplementary figures: 5

Abstract

Peach is a climacteric species whose ripening is regulated by the plant hormone ethylene. A crosstalk mechanism with auxin is necessary to support climacteric ethylene synthesis. The homeostasis control of auxin is regulated also by the activity of peptide hormones (PHs), acting both as short and long distant ligands. In this work, we investigated the role of *CTG134*, a peach gene encoding a GOLVEN-like PH isolated in mesocarp at the onset of ripening.

In peach fruit, *CTG134* was expressed during the climacteric transition and its mRNA level was induced by auxin and 1-methylcyclopropene (1-MCP) treatments, whereas it was minimally affected by ethylene. To better elucidate its function, *CTG134* was overexpressed in *Arabidopsis* and tobacco, which showed abnormal root hair growth, similar to wild-type plants treated with a synthetic form of the peptide. Molecular surveys demonstrated an impaired hormonal crosstalk, resulting in a re-modulated expression of a set of genes involved in both ethylene and auxin domains. In addition, the promoter of pCTG134 fused with GUS reporter highlighted gene activity in plant organs in which the auxin-ethylene interplay is known to occur. These data support the role of pCTG134 as mediator in an auxin-ethylene regulatory circuit.

Key words: 1-methylcyclopropene (1-MCP); *Arabidopsis thaliana;* CLE-LIKE (CLEL); GOLVEN (GLV); *Nicotiana tabacum;* peptide hormone; *Prunus persica*; ROOT GROWTH FACTOR (RGF); root hair

Introduction

In Angiosperms, fruits, besides providing essential and beneficial compounds to the human diet, protect the seeds enabling their dispersion at the end of the ripening phase. These organs originally develop from the ovary, with the possible contribution of other flower parts. According to the physiological regulation of ripening, fleshy fruits can be distinguished into climacteric (such as tomato, peach and apple) and non climacteric (such as strawberry, grape and citrus), depending on the presence of a burst in the production of the plant hormone ethylene accompanied by a respiratory increase occurring at the late stage of fruit ripening (Liu *et al.*, 2015). Ethylene is produced through the sequential activation of two biosynthetic systems (McMurchie *et al.*, 1972; Oetiker *et al.*, 1997). The auto-inhibitory system 1, found in both climacteric and non-climacteric fruit, maintains a basal level of ethylene during the vegetative growth of plants as well as in wound and stress response. The autocatalytic system 2 produces, instead, a much larger amount of the hormone, typical of climacteric fruits in full-ripening phase. In the tomato model, the switch between the two systems is based upon the differential expression of 1-amino-cyclopropane-1-carboxylic acid (ACC) synthase (ACS) and ACC oxidase (ACO) genes during the ripening process (Barry *et al.*, 2000). The transition from the system 1 to system 2, which represents a crucial point in the ripening process of climacteric species (Cara and Giovannoni, 2008), is also regulated by genetic (Vrebalov *et al.*, 2002; Manning *et al.*, 2006) and epigenetic factors (Zhong *et al.*, 2013), together with the surrounding environmental effect and interplay with other plant hormones (Klee and Giovannoni, 2011).

Emerging evidence suggests that relative functions of plant hormones are not restricted to a particular stage only. A complex network of more than one plant hormone is therefore involved in controlling various aspects of fruit development (Kumar *et al.*, 2014). The knowledge of the hormonal network and crosstalk relationship between different hormones during the stages of the fruit life cycle is still far from being complete (Kumar *et al.*, 2014) and relies almost entirely on model species (*Arabidopsis* and tomato). The action of the phytohormones depends not only on the cellular context, but also on the relationship established among different hormones. To date, the hormonal crosstalk has been mainly investigated in *Arabidopsis*, which shed light, among others, on the

113 crosstalk between auxin and ethylene (Poel *et al.*, 2015). The first and most
114 evident effect of the interaction between these two hormones is on the
115 regulation of the root morphogenesis process. Indeed, in this organ it has been
116 demonstrated that root hair formation, elongation (Pitts *et al.*, 1998; Dolan,
117 2001) and differentiation as well as the development of lateral roots are
118 regulated by the interplay occurring between auxin and ethylene (Zhang *et al.*,
119 2016). On the other hand, ethylene can also modify the auxin patterning by
120 modulating IAA transport (Prayitno *et al.*, 2006). Cellular and genetic evidences
121 have shown a physiological connection between hormones and peptide
122 hormones (PHs). ROOT GROWTH FACTOR/GOLVEN/CLE-Like
123 (RGF/GLV/CLEL) peptides can in fact alter auxin gradients by changing the
124 turnover of IAA carriers (Whitford *et al.*, 2012). Despite the importance of this
125 regulatory mechanism, the biology of PHs is still in its infancy, especially in non-
126 model but agronomically relevant species.
127 Auxin and ethylene have been described to interact at the level of ethylene
128 biosynthesis (Abel *et al.*, 1995) not only in *Arabidopsis* roots but also during the
129 ripening of different fruit species, such as tomato (Abel *et al.*, 1996), peach
130 (Trainotti *et al.*, 2007) and apple (Shin *et al.*, 2015). Although the molecular
131 mechanisms of the interplay between auxin and ethylene during fruit ripening
132 are still unknown, recent data suggest that PHs (Matsubayashi, 2014;
133 Tavormina *et al.*, 2015) could be the crossroads between the two hormones in
134 peach (Tadiello *et al.*, 2016). One PH in particular, namely CTG134 GLV-like,
135 was identified through a comprehensive survey carried out with the µPeach1.0
136 (Tadiello et al. 2016). This gene was expressed at the transition step between
137 the preclimacteric and the climacteric stage. Moreover, while CTG134 was
138 induced by exogenous treatment of 1-methylcyclopropene (1-MCP), an
139 ethylene competitor largely used to delay the normal physiological ripening
140 progression (Watkins, 2006), its expression was also totally repressed in ripe
141 fruit of *stony hard*, a peach mutant showing impairment both in ethylene
142 production and cell wall metabolism (Pan *et al.*, 2015).
143 In this work the peptide pCTG134, isolated from peach, was functionally
144 validated in *Arabidopsis* and tobacco, providing new evidence about its role as
145 a major regulator in the auxin-ethylene crosstalk.
146

147 **Materials and methods**

148 ***Plant materials***

149 Peach fruit s were collected from cv. 'Redhaven' (RH) as described in Tadiello
150 *et al*. (2016). The heterologous CTG134 overexpression was carried out in
151 *Arabidopsis* and tobacco plants. Seeds of *Arabidopsis thaliana* Columbia
152 accession (Col-0) were surface-sterilized, stratified overnight at 4°C and
153 germinated on plant growth medium (Murashige and Skoog, 1962) or in potting
154 soil at 22°C. To characterize root growth, MS plates were tilted with an angle of
155 45°. *Nicotiana tabacum* SNN plants were instead grown following standard
156 protocols in controlled greenhouse.

157 ***Hormone treatments on Redhaven fruit***

158 The auxin treatment was performed by dipping the whole fruit in 1-naphthalene
159 acetic acid [NAA, 2 mmol L^{-1} added with Silwet L-77 (200 µL L^{-1}) as surfactant]
160 for 15 min; thereafter, fruit were sprayed with the NAA solution every 12 h over
161 a period of 48 h (NAA omitted in the mock control). The ethylene treatment was
162 instead carried out as previously described in (Tadiello *et al.*, 2016).

163 ***1-MCP treatments on Stark Red Gold fruit***

164 Treatment of cv. "Stark Red Gold" (SRG) peach fruits with 1-MCP was carried
165 out as described in Tadiello *et al*. (2016).

166 ***RNA extraction and expression analyses by quantitative Real time PCR***
167 ***(qRT-PCR)***

168 Peach RNA was prepared from a frozen powder obtained by grinding mesocarp
169 sectors from at least four different fruits. From four grams of this powder, total
170 RNA was extracted following a protocol previously described (Chang *et al.*,
171 1993). *Arabidopsis* RNA was extracted from wild type and 35S::CTG134 mutant
172 seedlings, using the LiCl method (Verwoerd *et al.*, 1989). Expression analyses
173 were performed using Power SYBR Green PCR Master Mix (Applied
174 Biosystems). Normalization was performed using UBIQUITIN10 (UBI10) and
175 ACTIN8 as internal standards for Arabidopsis and
176 Ppa009483m/Prupe.8G137600 for peach (Primers are listed in Table S1). qRT-
177 PCR was performed and the obtained data analysed as previously described
178 (Tadiello *et al.*, 2016).

179 ***In-situ hybridizations***

180 *Prunus persica* S3II and S4 fruits were fixed and embedded in 4%
181 paraformaldehyde. A *CTG134* specific probe was amplified by PCR from S3II
182 and S4 fruit cDNAs (primers listed in Table S1) and further cloned in pGEM T-
183 easy vector (Promega). The CTG134 transformed vector was further used as
184 template for the creation of sense and antisense probes by an *in-vitro*
185 transcription performed with SP6 and T7 polymerases. Sections of plant tissue
186 were probed with dioxigenin-labelled antisense RNA-probe as previously
187 described (Brambilla *et al.*, 2007) and observed with a Zeiss Axiophot D1 light
188 microscope (http://www.zeiss.com).

189 ***pPR97-proCTG134:GUS construct design***

190 To assess the CTG134 promoter activity, a fragment of 2679 bp located
191 upstream of the coding sequence initiation site (Supplementary Fig. S1A) was
192 isolated from peach genomic DNA (cv Red Haven) by PCR. PCR product was
193 cloned into the pCR8/GW/TOPO TA Cloning vector (Invitrogen, Carlsbad, CA,
194 USA), according to the manufacturer's instructions and confirmed by
195 sequencing. The promoter fragment was thus subcloned into a pPR97-derived
196 vector (12.20 kb), made compatible with the Gateway cloning system (LR
197 Clonase II – Invitrogen, Carlsbad, CA, USA). This modified pPR97 vector with
198 kanamycin resistance was employed for stable transformations both in
199 *Arabidopsis thaliana* and *Nicotiana tabacum*, to measure the CTG134 promoter
200 activity. The promoter was tested by cloning the upstream sequence and a GUS
201 reporter gene interrupted by a plant intron (Vancanneyt *et al.*, 1990). To make
202 easier the cloning, a CC_rfA gateway cassette was inserted (SmaI) upstream of
203 the reporter gene and the antibiotic kanamycin was used to select resistant
204 successfully transformed plants.

205 ***pGreen-AmpR-KanNos-35S:CTG134 construct design***

206 The CTG134 coding sequence (524 bp) was amplified by PCR from *Prunus*
207 *persica* (cv Red Haven, S4I development stage) cDNA and subsequently
208 cloned into the pCR8/GW/TOPO TA Cloning vector (Invitrogen, Carlsbad, CA,
209 USA). The CTG134 CDS was further inserted into a pGreen-derived vector
210 (Hellens *et al.*, 2000) with the Gateway cloning system (LR Clonase II –
211 Invitrogen, Carlsbad, CA, USA). The pGreen-derived vector was modified to

212 confer resistance to both kanamycin and ampicillin. Moreover, a CC_rfA
213 gateway cassette was inserted downstream of the 35S promoter in the EcoRV
214 site. As before, the selection of plants was carried out with kanamycin
215 (Supplementary Fig. S1B).

216 ***Arabidopsis thaliana and tobacco transformation***

217 Single PCR-positive *Agrobacterium* GV3101 colonies were used to grow liquid
218 cultures for the transformation of *Arabidopsis thaliana* Columbia 0 plants with
219 the floral dip method (Clough and Bent, 1998). The first flowers of four-weeks
220 old plants were cut to allow, after 4-8 days, the growing of a second set, further
221 dipped in a suspension of *Agrobacterium* cells (OD_{600} = 0.8), sucrose (5% m/v)
222 and Silwet L-77 (0.05%). Plants were incubated in the dark for 16 hours before
223 a second growing phase in growth chamber (16/8 light/dark cycle, 25°C, 70%
224 relative humidity) until seeds were obtained. Transformed plants were screened
225 on solid ½ MS medium (MS salts with vitamins 2.17 g/L, sucrose 15 g/L, pH
226 5.75) supplemented with kanamycin (50 mg L^{-1}). After one week, the resistant
227 plants were planted into soil and grown in greenhouse for at least two
228 generations, until T-DNA insertions reached homozygosity. Plants were
229 screened for the presence of the transgene by PCR on genomic DNA using
230 specific primer pairs.

231 In-vitro grown *N. tabacum* SNN plants were instead transformed following the
232 protocol reported by (Fisher and Guiltinan, 1995). As for Arabidopsis, plants
233 were screened for the presence of the transgene with PCR on genomic DNA
234 using specific primer pairs.

235 ***Peptide synthesis***

236 The peptides DYSPARRKPPIHN and DY(SO_3H_2)SPARRKPPIHN were
237 synthesized by automatic solid phase procedures. The synthesis was
238 performed using a multiple peptide synthesizer (SyroII, MultiSynTech GmbH) on
239 a pre-loaded Wang resin (100-200 mesh) with N-α-Fmoc-N-β-trityl-l-asparagine
240 (Novabiochem, Bad Soden, Germany). The fluoren-9-ylmethoxycarbonyl
241 (Fmoc) strategy (Fields and Noble, 1990) was used throughout the peptide
242 chain assembly, utilizing O-(7-azabenzotriazol-1-yl)-N,N,N′,N′-
243 tetramethyluronium hexafluorophosphate (HATU) as coupling reagent (Carpino
244 *et al.*, 2001). The side-chain protected amino acid building blocks used were: N-

245 α-Fmoc-β-tert-butyl-l-aspartic acid, N-α-Fmoc-Nε-tert-butyloxycarbonyl-l-lysine,
246 N-α-Fmoc-Nω-2,2,4,6,7-pentamethyldihydrobenzofuran-5-sulfonyl-l-arginine, N-
247 α-Fmoc-O-tert-butyl-l-serine, N-α-Fmoc-N(im)-trityl-l-histidine, N-α-Fmoc-O-tert-
248 butyl-l-tyrosine and N-α-Fmoc-O-sulfo-l-tyrosine tetrabutylammonium salt.
249 Cleavage of the peptides was performed by incubating the peptidyl resins with
250 trifluoroacetic acid/H2O/triisopropylsilane (95%/2,5% /2,5%) for 2.5 h at 0 °C.
251 Crude peptides were purified by a preparative reverse phase HPLC. Molecular
252 masses of the peptide were confirmed by mass spectroscopy on a MALDI TOF-
253 TOF using a Applied Biosystems 4800 mass spectrometer.

254 ***Ca^{2+} measurement assays***

255 Ca^{2+} measurement assays were carried out in *Arabidopsis* cell suspension
256 cultures obtained from *Arabidopsis* seedlings stably expressing cytosolic
257 aequorin (seeds kindly provided by M.R. Knight, Durham, UK). Reconstitution of
258 aequorin and Ca^{2+} measurements were carried out as described (Sello *et al.*,
259 2016).

260 **Results**

261 ***Regulation of CTG134 expression***

262 Expression of *CTG134* was assessed in peach mesocarp during the onset of
263 fruit ripening (i.e. at early stage 4 –S4I – Fig. 1A). CTG134 mRNA accumulated
264 in preclimacteric fruit (i.e. S3II) after auxin treatment, while exogenous ethylene
265 had no effect (Fig. 1B). Moreover, treatment with the ethylene inhibitor 1-MCP
266 induced *CTG134* transcription at stages before (cl 0) and coincident (cl 1) with
267 the full climacteric (Fig. 1C). The peach mesocarp at ripening is mainly made up
268 of parenchymal cells and vascular tissue (Zanchin *et al.*, 1994). To localize the
269 types of cells expressing *CTG134* at ripening, *in-situ* hybridization experiments
270 were carried out with mesocarp sections prepared by peach fruit in S4 stage.
271 The CTG134 mRNA was localized in vascular bundles (Supplementary Fig.
272 S2C), most likely in the phloem or parenchymal cells (Fig. 1D).
273 Since peach is a recalcitrant species to transform, pro*CTG134:GUS* lines were
274 generated in both tobacco and *Arabidopsis* model species. In tobacco, a slight
275 but evident GUS staining was detected in the apical meristem (RAM) of *in-vitro*
276 grown lateral roots (Fig. 2A). Moreover, a dark staining was visible in lateral root
277 emergence (Fig. 2B) as well as in leaf, mainly associated, but not limited to, the

278 vascular tissue (Fig. 2C). In the stem of one-week-old plantlets, GUS
279 expression was localized in phloem of cell layers closed to the cambium (Fig.
280 2D). GUS expression was also tested in reproductive organs, where it was
281 detected in the tips of both young sepals and petals (not shown) and in
282 capsules at the level of the dehiscence zone (Fig. 2E). The inner part of the fruit
283 was the part more significantly stained (Figures 2F and 2G), with the highest
284 expression in the placenta (Fig. 2G). On the contrary, in all the transgenic lines
285 investigated in this study, the GUS colouration was never observed in ovule. In
286 one-week-old tobacco seedlings the reporter was more expressed in cotyledons
287 than roots. However, five-hour treatment with 50μM IAA induced a different
288 GUS staining in the entire shoot apex and root, reaching the highest intensity in
289 the root-stem transition zone (Fig. 2H). A similar auxin-induced expression was
290 also observed in roots of *in-vitro* grown plantlets (Fig. 2I). The stimulation of the
291 GUS staining in tobacco finds also consistency with the aforementioned
292 expression pattern of CTG134 in peach fruit. The expression of this element
293 was in fact enhanced by auxin (Fig. 1B) and auxin responsive elements (AREs)
294 were moreover detected in the *CTG134* promoter region (Supplementary Fig.
295 S1B). To further validate the heterologous analysis carried out in tobacco, the
296 activity of the CTG134 promoter was additionally investigated in *Arabidopsis*
297 (Fig. 3A). Also in this species, the GUS expression was higher in cotyledons
298 (Fig. 3B) rather than in primary root, where the GUS staining was undetectable
299 in the RAM (Fig. 3C). The GUS activity was instead clearly visible at the root-
300 stem transition zone (Fig. 3D) and during lateral root emergence (Fig. 3E). In
301 the reproductive organs, the expression pattern was detected in abscission
302 zones before (Fig. 3F) and after (Fig. 3G) shedding. The expression was also
303 detected in maturing siliques and leaves, especially in those associated with
304 vascular bundles (Fig. 3H).

305 ***4.2 Hormonal regulation of CTG134 in tobacco***

306 To test whether the auxin responsiveness was due to the promoter regulatory
307 region, one-week old tobacco seedlings of line #2 were exposed to increasing
308 concentrations of IAA. The CTG134 promoter was responsive to IAA already at
309 0.5μM, with an activity pattern proportional to the hormone concentrations. The
310 system reached saturation at 50μM (Fig. 4A). The IAA induction kinetic was
311 assessed over a time course of 20 hours on tobacco seedlings of line #2

312 treated with 10μM IAA. An initial slight induction in both control and treated
313 samples was observed already after 30 minutes, after which the GUS activity
314 remained at a basal level in the control, while in the IAA treated samples a
315 significant burst was observed after 3 hours after the treatment (Fig. 4B). Since
316 in peach fruit the expression of CTG134 was insensitive to ethylene and
317 induced by 1-MCP (Fig. 2B and 2C), the promoter responsiveness was tested
318 by treating ten-day-old tobacco seedlings for sixteen hours with ethylene (10μL
319 L^{-1}), IAA (10μM) and 1-MCP (1μL L^{-1}). 1-MCP induced the reporter activity
320 similarly to auxin (Fig. 4C), while treatment with ethylene did not change the
321 expression of the GUS reporter gene.

322 ***Over-expression of* CTG134 *in tobacco***

323 To functionally investigate the role of the peptide CTG134 peptide, its full-length
324 coding sequence, under the control of the Cauliflower mosaic virus 35S (35S
325 CaMV) promoter was expressed in tobacco. The development of longer root
326 hairs was noticed already in the early phases of transgenic plant production (Fig.
327 5A). A YFP gene, cloned in the same binary vector as CTG134, was
328 overexpressed to have control plants able to grow on kanamycin and
329 gentamicin present in the growth media. To further assess this phenotype,
330 scions from different clones were propagated and primary roots from 30 day-old
331 plants were analysed by taking images in the root portion located at 6 mm from
332 the root tip. On average, the CTG134 overexpressing lines showed an increase
333 of at least two-fold in root hair length (ANOVA, $F = 87.75$, $df = 155$, $p < 0.001$)
334 with respect to control wild type plants (Fig. 5B). The effect on root development
335 was also evident during adventitious roots formation in *in-vitro* plants
336 (Supplementary Fig. S3A and B). Indeed, root primordia emerged earlier in
337 *35S:CTG134* scions than in wild type, although the root growth was slower,
338 resulting at the end in shorter roots (Supplementary Fig. S3C). Within the
339 hypothesis of the auxin-ethylene crosstalk, the putative mediating role of
340 CTG134 was investigated exposing 35S:CTG134 transformed tobacco plants to
341 ethylene (10μL L^{-1}) and grown in dark. As revealed by Environmental Scanning
342 Electron Microscopy (ESEM, Figures 5c-f), although the difference in the root
343 hair phenotype was confirmed, a clear distinction between transgenic lines and
344 controls for the apical hook and hypocotyl thickening, typical of the triple
345 ethylene response, was not observed. Indeed, the untreated (air) 35S:CTG134

346 (Fig. 5E) seedlings displayed a phenotype similar to those grown in presence of
347 ethylene (Fig. 5D), despite the fact that samples were partially dehydrated by
348 the light vacuum imposed during the ESEM observation. Interestingly, the
349 ethylene treatment induced an additional phenotype in the 35S:CTG134 lines,
350 provoking the development of a massive root hair formation, completely
351 wrapping the root body (Fig. 5F). Subsequently, a Scanning Electron
352 Microscopy (SEM) analysis disclosed that the previously observed root hair
353 phenotype was due to an increase of their density in the 35S:CTG134 lines (Fig.
354 5H) with regards to control (Fig. 5G). Indeed, most of the root epidermal cells of
355 35S:CTG134 seedlings developed root hairs, while in WT trichoblasts were
356 arranged in alternating files with atrichoblasts along the root surface.
357 Since the CTG134 sequence was originally isolated from peach fruit, and
358 placenta cells were stained in tobacco plants expressing the GUS reporter gene
359 driven by the CTG134 promoter, tobacco transgenic capsules were also
360 analysed. Even if tobacco produces a dry fruit structurally different from the
361 fleshy stone fruit of peach, the CTG134 overexpression led to a detectable
362 effect. Tobacco capsules of 35S:CTG134, harvested 12 days after anthesis
363 (before drying), showed an increase in diameter of about 16% with respect to
364 wild type or 35S:YFP (ANOVA, F = 3,85, df = 22, p = 0.013) (Supplementary
365 Fig. S4).

366 ***Over-expression of* CTG134 *in Arabidopsis***

367 Similarly to tobacco, the same construct was further employed to transform
368 *Arabidopsis*. T2 CTG134 overexpressing lines were easily identified for their
369 root phenotype when grown on horizontal plates. The primary root of five-day-
370 old 35S:CTG134 seedlings had indeed longer hairs than WT ones (Fig. 6A).
371 Moreover, root hairs developed closer to the apex that in WT roots. To quantify
372 the latter effect, the hairless portion of the root was about half (ANOVA, F =
373 101.1, df = 23, p < 0.001) of that in the WT (Fig. 6B). As regards to root hair
374 length, being not uniform along the root and clearly depending on age, sizes
375 were taken at given distances from the root-stem transition zone and in a region
376 of the tip that was determined to be, based on growth rate, four-day old. Both
377 measures clearly indicated that the root hairs in the overexpressing lines were
378 longer (ANOVA, F = 95.07, df = 342, p < 0.001; ANOVA, F = 98.31, df = 342, p
379 < 0.001, respectively) than wild type (Fig. 6C). Members of the RGF/GLV family

380 in *Arabidopsis* are known to induce developmental defects in roots when over-
381 expressing seedlings were grown on tilted plates, as reported by (Whitford *et al.*,
382 2012; Fernandez *et al.*, 2013). Accordingly, in this work *Arabidopsis*
383 35S:CTG134 seedlings produced roots with larger and more irregular waves
384 than the WT (Fig. 6D). This effect could be phenocopied by the WT when the
385 synthetic CTG134 peptide (pCGT134) was added to the medium, with the
386 sulfated form being more active than the non-sulfated one (Fig. 6D). Albeit the
387 hairless portion of the root was shorter in overexpressing seedlings, the
388 meristematic region of the root was longer. Moreover, both 35S:CTG134 lines
389 and WT seedlings grown in a medium supplemented with pCTG134 had an
390 increase in root meristem size (Figures 6E and F). The effect on the root
391 meristem size was saturable, as overexpressing lines did not respond to
392 exogenous pCTG134 as the WT (Fig. 6F).
393 The effect of *CTG134* overexpression at the transcriptional level was tested on
394 five-day-old seedling roots (Fig. 7). Alteration in root hairs morphology and
395 quantity was accompanied with a reduction of *GLABRA2* (*GL2*) and a slight
396 induction of *CAPRICE* (*CPC*) expression. The increased meristem size was
397 supported by the expression of *CYCLIN B1;1* (*CYCB1;1*). The development of
398 root hair was selected as a suitable developmental process to test the effect of
399 CTG134 on the interactions between ethylene and auxin occurring at the onset
400 of peach ripening, since the crosstalk of the two hormones during root hair
401 development is well documented (reviewed by Poel *et al.* 2015). The expression
402 of the ethylene biosynthetic gene *ACS2* was induced in roots of 35S:CTG134
403 seedlings (Fig. 7), as well as that of *ETR1* and *EIN3*, encoding an ethylene
404 receptor and a transcription factors starting the transcriptional cascade leading
405 to ethylene responses, respectively. On the contrary, transcription of *CTR1*,
406 encoding the first downstream signalling component after the ethylene
407 receptor(s) (Kieber *et al.*, 1993) was unaffected (Supplementary Fig. S5). About
408 auxin, both *TAA1* and *YUC3* and *6* genes involved in the indole-3-pyruvic acid
409 branch of the hormone synthesis pathway (Tivendale *et al.*, 2014) were induced
410 in *CTG134* overexpressing seedlings, while *AMI1*, involved in the indole-3-
411 acetamide branch of the pathway, seemed unaffected (Figures 7 and S5). Free
412 auxin levels depend not only on hormone synthesis but also on its release from
413 storage compartments and transport. The expression of *IAR3*, a gene encoding

414 an IAA-Ala hydrolase (Davies *et al.*, 1999), decreased in *CTG134*
415 overexpressing plants, while *PIN2*, encoding an auxin efflux carrier (Müller *et al.*,
416 1998) was induced (Fig. 7).

417 ***pCTG134 induces a cytosolic Ca^{2+} change***

418 In peach, a gene encoding a Ca^{2+} sensing protein belonging to the Calcineurin
419 B-like (CBL) family (*CTG85*) mirrored the expression of *CTG134* during fruit
420 ripening, as well as after 1-MCP treatment (Tadiello *et al.*, 2016). The
421 expression of *CBL1*, *2*, *4*, and *10* encoding genes was therefore tested in
422 35S:CTG134 roots, showing a general repression, with *CBL2* as the most
423 severely down-regulated gene (Figures 7 and S5).
424 Given the effect on CBL gene expression and the potential involvement of Ca^{2+}
425 in the signalling pathway activated by signalling peptides (Ma *et al.*, 2013),
426 *Arabidopsis* cell suspension cultures stably expressing the bioluminescent Ca^{2+}
427 reporter aequorin in the cytosol were challenged with 100 μM pCTG134. Ca^{2+}
428 measurement assays demonstrated the induction of a biphasic cytosolic Ca^{2+}
429 transient, characterized by a rapid rise, which equally quickly dissipated,
430 followed by a slower Ca^{2+} increase, peaking at about 0.5 μM after 100 s and
431 falling back to basal levels within 5 min (Fig. 8A). No changes in cytosolic Ca^{2+}
432 concentration ($[Ca^{2+}]_{cyt}$) were detected in response to either plant cell culture
433 medium (Fig. 8B) or a non-specific peptide (100 μM T16E S19A2) (Fig. 8C),
434 supporting the specificity of the observed Ca^{2+} response to the sulfated
435 CTG134 peptide.

436 **Discussion**

437 Peptide hormones participate in both proximal and distal cell-to-cell
438 communication processes necessary during growth as well as to cope with
439 biotic and abiotic stimuli (reviewed in (Matsubayashi, 2014; Tavormina *et al.*,
440 2015; Wang *et al.*, 2016). Despite the growing interest in peptide hormones,
441 their possible role during fleshy fruit ripening remains almost unexplored (Zhang
442 *et al.*, 2014). In peach fruit, gene expression profiling suggested that *CTG134*,
443 encoding a peptide belonging to the RGF/GLV family, could be involved in the
444 crosstalk between auxin and ethylene occurring at the onset of fruit ripening
445 (Tadiello *et al.*, 2016).

446 ***CTG134 expression is ripening specific and affected by auxin and***
447 ***ethylene perception***
448 Extensive RNA profiling confirmed that *CTG134* is expressed almost exclusively
449 at the onset of ripening, during the transition stage from system 1 to 2 (Fig. 1),
450 as initially suggested by Tadiello *et al.* (2016).
451 Considering the difficulties typical of *Prunus* species during the *in vitro*
452 regeneration phase, tobacco and *Arabidopsis* transgenic lines expressing the
453 GUS reporter gene driven by the CTG134 promoter sequence, were created.
454 The cis-regulatory elements present in the peach *CTG134* promoter drive *GUS*
455 gene expression in cell/tissue types where the crosstalk between auxin and
456 ethylene was described both in tobacco (Fig. 2) and *Arabidopsis* (Fig. 3). These
457 comprise both cells undergoing separation processes, like abscission,
458 dehiscence zones, lateral root primordia (Roberts *et al.*, 2002; Kumpf *et al.*,
459 2013), cambium associated cells (Love *et al.*, 2009; Sanchez *et al.*, 2012) and
460 placenta cells (De Martinis and Mariani, 1999; Pattison *et al.*, 2015). The
461 specificity of the GUS staining pattern obtained in heterologous systems was
462 validated by *in-situ* hybridization in peach mesocarp, where *CTG134* expression
463 was more abundant in bundle associated cells (Fig. 1d). It is noteworthy that
464 also regulatory regions of tomato (Blume and Grierson, 1997), apple (Atkinson
465 *et al.*, 1998) and peach (Moon and Callahan, 2004) *ACO* genes drove GUS
466 expression more abundantly in bundle than parenchyma cells of tomato
467 pericarp. Besides spatial regulation, also hormone responsiveness within
468 *CTG134* regulatory regions supported the role in the crosstalk between auxin
469 and ethylene (Fig. 1 and 4). Indeed, both on ripening mesocarp and tobacco
470 seedlings, not only IAA had an inductive effect, probably due to the presence of
471 AREs, but also the altered perception of ethylene (due to 1-MCP treatment)
472 stimulated both *CTG134* transcription in ripening fruit and *GUS* accumulation in
473 tobacco seedlings. In ripening peaches 1-MCP induced auxin synthesis
474 (Tadiello *et al.*, 2016), and this might be the reason of the *CTG134* induction. 1-
475 MCP treatment might have induced IAA synthesis, and thus GUS expression,
476 also in tobacco seedlings. In roots of *Arabidopsis* treated with silver (also
477 blocking the perception of ethylene; Negi *et al.* 2008) the exogenous application
478 of 1-MCP might have altered the distribution of IAA, leading to *GUS* induction.

479 ***35S:CTG134 plants show phenotypes related to auxin and ethylene action***
480 When *CTG134* was permanently overexpressed in tobacco and *Arabidopsis*
481 plants (Figures 5 and 6), the most striking effect was related to the length and
482 number of root hairs, mimicking the effect of exogenous treatments with auxin
483 or ethylene (Pitts *et al.*, 1998). Adventitious root formation and elongation in
484 tobacco were also affected, as well as capsule size, further supporting the
485 interplay between auxin and ethylene actions. Besides the well-known effect on
486 root hair number and morphology reported for RGF/GLV/CLEL (Whitford *et al.*,
487 2012; Fernandez *et al.*, 2013) and CLE peptides (Fiers *et al.*, 2005), CTG134
488 had an impact also on tobacco capsule size. In fact, at maturity, tobacco
489 capsules were 16% larger than WT on average, similarly to carnation flowers
490 treated with ethylene (Nichols, 1976). Ethylene synthesis is necessary for
491 normal ovule development which impacts flower size (De Martinis and Mariani,
492 1999). The GUS staining in tobacco placenta and the larger capsules in
493 CTG134 overexpressing plants allow therefore to hypothesize that CTG134
494 may corroborate auxin inductive and ethylene repressive actions during fruit
495 setting (Martínez *et al.*, 2013; Shinozaki *et al.*, 2015).

496 ***Molecular targets of CTG134 and its role as mediator in the auxin/ethylene***
497 ***crosstalk***
498 The *Arabidopsis* root model was moreover exploited to gain insights into the
499 regulatory circuit associating CTG134 with auxin and ethylene (Figures 6 and 7).
500 The wavy root phenotype and the increase in meristem size were observed in
501 both overexpressing and peptide treated seedlings, confirming previous findings
502 (Matsuzaki *et al.*, 2010; Whitford *et al.*, 2012). The observed increase in the
503 meristem size was also supported by the induced expression of *CYCB1;1* (Fig.
504 7), while the down-regulation of *GL2* was in agreement with its repressing role
505 in root hair development (Ishida *et al.*, 2008). More interestingly, genes of both
506 auxin and ethylene synthesis, transport and transduction pathways were
507 upregulated in CTG134 overexpressing roots, assigning to this RGF/GLV
508 peptide a role in the auxin/ethylene crosstalk (Stepanova *et al.*, 2007). Although
509 we did not carry out a detailed analysis on the effects caused by the local
510 application of CTG134 peptide (that in Arabidopsis controlled the PIN2
511 abundance in the root meristem by a post-transcriptional mechanism, thus
512 guiding auxin distribution; Whitford *et al.*, 2012), we showed that the

513 heterologous overexpression of the peach CTG134 peptide could be sensed in
514 the portion of the root where receptors initiate the signalling cascade
515 (Shinohara *et al.*, 2016; Ou *et al.*, 2016; Song *et al.*, 2016). As for Peps
516 signalling in *Arabidopsis* (Ma *et al.*, 2013), aequorin-based Ca^{2+} measurement
517 assays (Fig. 8) demonstrated the induction by the sulfated peptide CTG134 of a
518 remarkable cytosolic Ca^{2+} change, suggesting the likely involvement of Ca^{2+} as
519 intracellular messenger in the transduction pathway activated by this signal
520 peptide. The role of Ca^{2+} is supported also by the downregulation of several
521 CALCINEURIN B-LIKE PROTEIN (CBL) genes in roots of CTG134
522 overexpressing seedlings, in agreement with the downregulation of a CBL gene
523 in 1-MCP-treated peaches (Tadiello *et al.*, 2016). Sensing the peptide also
524 induced the transcription of key genes of ethylene and auxin biosynthesis
525 pathways and thus, reasonably, the levels of these two hormones, which
526 eventually led to the observed phenotypes. While the response in the ethylene
527 pathway is somewhat straightforward investigating the induction of key genes in
528 its synthesis (*ACS2*), perception (*ETR1*) and signal transduction (*EIN3*), the
529 action on the auxin pathway is more intricate. Indeed, while the increased
530 transcription of *TAA1*, *YUC3* and *YUC6* sustains the induction of the two-step
531 IPA pathway, the unchanged levels of *AMI1* seemed to exclude the conversion
532 of indole-3-acetamide (IAM) to IAA (Enders and Strader, 2015). Moreover,
533 although only *IAR3* was tested, the contribution of conjugated forms of IAA
534 (Sanchez Carranza *et al.*, 2016) seemed negligible in *Arabidopsis*, while the
535 expression of its peach homolog *CTG475* was supposed to participate to the
536 free auxin increase measured before the climacteric production of ethylene in
537 peach (Tadiello *et al.*, 2016), thus complementing the role of *PpYUC11* (Pan *et*
538 *al.*, 2015). However, the induced transcription of *PIN* genes in overexpressing
539 *Arabidopsis* seedlings (Fig. 7) and in climacteric peaches (Tadiello *et al.*, 2016)
540 supported a key role of these peptides in regulating auxin distribution (Whitford
541 *et al.*, 2012).
542 The comprehensive expression profiling data carried out in peach (Tadiello *et*
543 *al.*, 2016) and the knowledge here achieved about CTG134 in tobacco and
544 *Arabidopsis* provide evidence on the involvement of this RGF/GVL secreted
545 peptide in a regulatory circuit that sustains auxin and ethylene actions. The
546 same circuit, working in both rosids (*Arabidopsis*) and asterids (tobacco) might

547 have appeared early during evolution of eudicots to participate in the control of
548 root hair development and later it could have been recruited in peach to
549 regulate the switch from system 1 to system 2 ethylene synthesis (Fig. 9).
550 Further research will be necessary to clarify the molecular details by which
551 CTG134 acts to either regulate auxin and ethylene synthesis or modify their
552 distribution and perception, or both. The kinase nature of GLVs receptors
553 (Shinohara *et al.*, 2016; Ou *et al.*, 2016; Song *et al.*, 2016) agrees with the
554 measured Ca^{2+} perturbations.
555 The unique mechanism that switches ethylene synthesis from system 1 to
556 system 2 in peach probably relies on the use of a single ACS gene for both
557 kinds of syntheses (Tadiello *et al.*, 2016), thus differing from tomato (Barry *et al.*,
558 2000) and apple (Wang *et al.*, 2009). In these two latter fruits, the expression of
559 *LeACS4* and *MdACS3* (system 1) is necessary to start *LeACS2* and *MdACS1*
560 transcription (system 2), respectively. During peach ripening, expression of
561 other ACS genes is, if present, several orders of magnitude lower than that of
562 *ACS1* (Tadiello *et al.*, 2016). The different amount of ethylene released by
563 system 1 and system 2 could be achieved by modulating system 1 ACS1
564 activity, thus leading to system 2 *ACS1* increased transcription. ACS1 belongs
565 to type-1 ACS proteins, which are stabilized by phosphorylation mediated by
566 mitogen-activated protein kinases (MAPKs) (Liu and Zhang, 2004).
567 Phosphorylation cascades have been shown to start upon binding of peptide
568 signals (e.g. IDA) with their receptors (e.g. HAE/HSL2) (Cho *et al.*, 2008). Given
569 the transcriptional regulation of *CTG134*, the nature of pCTG134 and of the
570 *Arabidopsis* receptors of its homologous RGF/GLV peptides (Shinohara *et al.*,
571 2016; Ou *et al.*, 2016; Song *et al.*, 2016) and of the ability of pCTG134 to trigger
572 a cytosolic Ca^{2+} signal, we hypothesized that the transition of ethylene
573 synthesis from system 1 to system 2 in peach could be controlled by ACS1,
574 whose activity might be therefore modulated through the action of pCTG134.

575 **Supplementary Data**

576

577 **Fig. S1.** Details of the vectors used for gene overexpression and promoter
578 analyses.

579

580 **Fig. S2.** Localization of *CTG134* expression in peach mesocarp by *in-situ*

581 hybridization (control panels).
582
583 **Fig. S3.** Adventitious root formation in 35S:CTG134 clones and in control lines.
584
585 **Fig. S4.** Effects on capsule size of *CTG134* overexpression in tobacco.
586
587 **Fig. S5** Relative expression profiles of selected genes in roots of *Arabidopsis*
588 seedlings grown on agar plates for five days.
589
590 **Table S1** List and sequences of DNA primers used.
591

592 **Acknowledgements**
593 We thank M.R. Knight (Durham, UK) and G. Regiroli (AgroFresh Inc.,
594 Philadelphia, PA, USA) for kindly providing seeds of aequorin-expressing
595 Arabidopsis plants and SmartFreshTM (1-MCP), respectively. The authors are
596 also grateful to Alice Tadiello and Maria Patrizia Schiappelli for providing
597 preliminary expression data and support in peptide synthesis. Financial support
598 was provided by MIUR (Italian Ministry of Research and University), MiPAFF
599 (Ministero delle Politiche Agricole Alimentari e Forestali–Italy;
600 www.politicheagricole.it) through the project 'DRUPOMICS' (grant
601 DM14999/7303/08) and the University of Padova (grant CPDA072133/07 and
602 CPDA132841/13) to LT.

References

Abel S, Ballas N, Wong L-M, Theologis A. 1996. DNA elements responsive to auxin. BioEssays **18**, 647–654.
Abel S, Nguyen MD, Chow W, Theologis A. 1995. ASC4, a Primary Indoleacetic Acid-responsive Gene Encoding 1-Aminocyclopropane-1-carboxylate Synthase in Arabidopsis thaliana STRUCTURAL CHARACTERIZATION, EXPRESSION IN ESCHERICHIA COLI, AND EXPRESSION CHARACTERISTICS IN RESPONSE TO AUXIN. Journal of Biological Chemistry **270**, 19093–19099.
Atkinson RG, Bolitho KM, Wright MA, Iturriagagoitia-Bueno T, Reid SJ, Ross GS. 1998. Apple ACC-oxidase and polygalacturonase: ripening-specific gene expression and promoter analysis in transgenic tomato. Plant molecular biology **38**, 449–460.
Barry CS, Llop-Tous MI, Grierson D. 2000. The regulation of 1-aminocyclopropane-1-carboxylic acid synthase gene expression during the transition from system-1 to system-2 ethylene synthesis in tomato. Plant Physiology **123**, 979–986.
Blume B, Grierson D. 1997. Expression of ACC oxidase promoter—GUS fusions in tomato and Nicotiana plumbaginifolia regulated by developmental and environmental stimuli. The Plant Journal **12**, 731–746.
Brambilla V, Battaglia R, Colombo M, Masiero S, Bencivenga S, Kater MM, Colombo L. 2007. Genetic and Molecular Interactions between BELL1 and MADS Box Factors Support Ovule Development in Arabidopsis. The Plant Cell **19**, 2544–2556.
Cara B, Giovannoni JJ. 2008. Molecular biology of ethylene during tomato fruit development and maturation. Plant Science **175**, 106–113.
Carpino LA, Henklein P, Foxman BM, Abdelmoty I, Costisella B, Wray V, Domke T, El-Faham A, Mügge C. 2001. The solid state and solution structure of HAPyU. The Journal of Organic Chemistry **66**, 5245–5247.
Chang S, Puryear J, Cairney J. 1993. A simple and efficient method for isolating RNA from pine trees. Plant Molecular Biology Reporter **11**, 113–116.
Cho SK, Larue CT, Chevalier D, Wang H, Jinn T-L, Zhang S, Walker JC. 2008. Regulation of floral organ abscission in Arabidopsis thaliana. Proceedings of the National Academy of Sciences **105**, 15629–15634.
Clough SJ, Bent AF. 1998. Floral dip: a simplified method for Agrobacterium-mediated transformation of Arabidopsis thaliana. The Plant Journal: For Cell and Molecular Biology **16**, 735–743.
Davies RT, Goetz DH, Lasswell J, Anderson MN, Bartel B. 1999. IAR3 encodes an auxin conjugate hydrolase from Arabidopsis. The Plant Cell **11**, 365–376.
De Martinis D, Mariani C. 1999. Silencing Gene Expression of the Ethylene-Forming Enzyme Results in a Reversible Inhibition of Ovule Development in Transgenic Tobacco Plants. The Plant Cell **11**, 1061–1072.
Dolan L. 2001. The role of ethylene in root hair growth in Arabidopsis. Journal of Plant Nutrition and Soil Science **164**, 141–145.
Enders TA, Strader LC. 2015. Auxin activity: Past, present, and future. American Journal of Botany **102**, 180–196.
Fernandez A, Andrzej Drozdzecki, Kurt Hoogewijs, Anh Nguyen, Tom Beeckman, Annemieke Madder, Pierre Hilson. 2013. Transcriptional and Functional Classification of the GOLVEN/ROOT GROWTH FACTOR/CLE-Like Signaling Peptides Reveals Their Role in Lateral Root and Hair Formation. Plant Physiology **161**, 954–970.
Fields GB, Noble RL. 1990. Solid phase peptide synthesis utilizing 9-

fluorenylmethoxycarbonyl amino acids. International Journal of Peptide and Protein Research **35**, 161–214.
Fiers M, Golemiec E, Xu J, Geest L van der, Heidstra R, Stiekema W, Liu C-M. 2005. The 14–Amino Acid CLV3, CLE19, and CLE40 Peptides Trigger Consumption of the Root Meristem in Arabidopsis through a CLAVATA2-Dependent Pathway. The Plant Cell **17**, 2542–2553.
Fisher DK, Guiltinan MJ. 1995. Rapid, efficient production of homozygous transgenic tobacco plants withagrobacterium tumefaciens: A seed-to-seed protocol. Plant Molecular Biology Reporter **13**, 278–289.
Hellens RP, Edwards EA, Leyland NR, Bean S, Mullineaux PM. 2000. pGreen: a versatile and flexible binary Ti vector for Agrobacterium-mediated plant transformation. Plant Molecular Biology **42**, 819–832.
Ishida T, Kurata T, Okada K, Wada T. 2008. A genetic regulatory network in the development of trichomes and root hairs. Annu. Rev. Plant Biol. **59**, 365–386.
Kieber JJ, Rothenberg M, Roman G, Feldmann KA, Ecker JR. 1993. CTR1, a negative regulator of the ethylene response pathway in arabidopsis, encodes a member of the Raf family of protein kinases. Cell **72**, 427–441.
Klee HJ, Giovannoni JJ. 2011. Genetics and Control of Tomato Fruit Ripening and Quality Attributes. Annual Review of Genetics **45**, 41–59.
Kumar R, Khurana A, Sharma AK. 2014. Role of plant hormones and their interplay in development and ripening of fleshy fruits. Journal of Experimental Botany **65**, 4561–4575.
Kumpf RP, Shi C-L, Larrieu A, Stø IM, Butenko MA, Péret B, Riiser ES, Bennett MJ, Aalen RB. 2013. Floral organ abscission peptide IDA and its HAE/HSL2 receptors control cell separation during lateral root emergence. Proceedings of the National Academy of Sciences **110**, 5235–5240.
Liu M, Pirrello J, Chervin C, Roustan J-P, Bouzayen M. 2015. Ethylene control of fruit ripening: revisiting the complex network of transcriptional regulation. Plant Physiology, pp.01361.2015.
Liu Y, Zhang S. 2004. Phosphorylation of 1-Aminocyclopropane-1-Carboxylic Acid Synthase by MPK6, a Stress-Responsive Mitogen-Activated Protein Kinase, Induces Ethylene Biosynthesis in Arabidopsis. The Plant Cell **16**, 3386–3399.
Love J, Björklund S, Vahala J, Hertzberg M, Kangasjärvi J, Sundberg B. 2009. Ethylene is an endogenous stimulator of cell division in the cambial meristem of Populus. Proceedings of the National Academy of Sciences **106**, 5984–5989.
Ma Y, Zhao Y, Walker RK, Berkowitz GA. 2013. Molecular Steps in the Immune Signaling Pathway Evoked by Plant Elicitor Peptides: Ca2+-Dependent Protein Kinases, Nitric Oxide, and Reactive Oxygen Species Are Downstream from the Early Ca2+ Signal. Plant Physiology **163**, 1459–1471.
Manning K, Tör M, Poole M, Hong Y, Thompson AJ, King GJ, Giovannoni JJ, Seymour GB. 2006. A naturally occurring epigenetic mutation in a gene encoding an SBP-box transcription factor inhibits tomato fruit ripening. Nature Genetics **38**, 948–952.
Martínez C, Manzano S, Megías Z, Garrido D, Picó B, Jamilena M. 2013. Involvement of ethylene biosynthesis and signalling in fruit set and early fruit development in zucchini squash (Cucurbita pepo L.). BMC plant biology **13**, 139.
Matsubayashi Y. 2014. Posttranslationally Modified Small-Peptide Signals in Plants. Annual Review of Plant Biology **65**, 385–413.
Matsuzaki Y, Ogawa-Ohnishi M, Mori A, Matsubayashi Y. 2010. Secreted Peptide Signals Required for Maintenance of Root Stem Cell Niche in Arabidopsis. Science **329**, 1065–1067.

McMurchie EJ, McGlasson WB, Eaks IL. 1972. Treatment of fruit with propylene gives information about the biogenesis of ethylene. Nature **237**, 235–236.
Moon H, Callahan AM. 2004. Developmental regulation of peach ACC oxidase promoter–GUS fusions in transgenic tomato fruits. Journal of Experimental Botany **55**, 1519–1528.
Müller A, Guan C, Gälweiler L, Tänzler P, Huijser P, Marchant A, Parry G, Bennett M, Wisman E, Palme K. 1998. AtPIN2 defines a locus of Arabidopsis for root gravitropism control. The EMBO journal **17**, 6903–6911.
Murashige T, Skoog F. 1962. A Revised Medium for Rapid Growth and Bio Assays with Tobacco Tissue Cultures. Physiologia Plantarum **15**, 473–497.
Negi S, Ivanchenko MG, Muday GK. 2008. Ethylene regulates lateral root formation and auxin transport in Arabidopsis thaliana. The Plant Journal **55**, 175–187.
Nichols R. 1976. Cell enlargement and sugar accumulation in the gynaecium of the glasshouse carnation (Dianthus caryophyllus L.) induced by ethylene. Planta **130**, 47–52.
Oetiker JH, Olson DC, Shiu OY, Yang SF. 1997. Differential induction of seven 1-aminocyclopropane-1-carboxylate synthase genes by elicitor in suspension cultures of tomato (Lycopersicon esculentum). Plant Molecular Biology **34**, 275–286.
Ou Y, Lu X, Zi Q, *et al.* 2016. RGF1 INSENSITIVE 1 to 5, a group of LRR receptor-like kinases, are essential for the perception of root meristem growth factor 1 in Arabidopsis thaliana. Cell Research **26**, 686–698.
Pan L, Zeng W, Niu L, *et al.* 2015. PpYUC11, a strong candidate gene for the stony hard phenotype in peach (Prunus persica L. Batsch), participates in IAA biosynthesis during fruit ripening. Journal of Experimental Botany **66**, 7031–7044.
Pattison RJ, Csukasi F, Zheng Y, Fei Z, Knaap E van der, Catalá C. 2015. Comprehensive Tissue-Specific Transcriptome Analysis Reveals Distinct Regulatory Programs during Early Tomato Fruit Development. Plant Physiology **168**, 1684–1701.
Pitts RJ, Cernac A, Estelle M. 1998. Auxin and ethylene promote root hair elongation in Arabidopsis. The Plant Journal **16**, 553–560.
Poel BV de, Smet D, Straeten DVD. 2015. Ethylene and Hormonal Cross Talk in Vegetative Growth and Development. Plant Physiology **169**, 61–72.
Prayitno J, Rolfe BG, Mathesius U. 2006. The Ethylene-Insensitive sickle Mutant of Medicago truncatula Shows Altered Auxin Transport Regulation during Nodulation. Plant Physiology **142**, 168–180.
Roberts JA, Elliott KA, Gonzalez-Carranza ZH. 2002. Abscission, Dehiscence, and Other Cell Separation Processes. Annual Review of Plant Biology **53**, 131–158.
Sanchez Carranza AP, Singh A, Steinberger K, Panigrahi K, Palme K, Dovzhenko A, Dal Bosco C. 2016. Hydrolases of the ILR1-like family of Arabidopsis thaliana modulate auxin response by regulating auxin homeostasis in the endoplasmic reticulum. Scientific Reports **6**, 24212.
Sanchez P, Nehlin L, Greb T. 2012. From thin to thick: major transitions during stem development. Trends in Plant Science **17**, 113–121.
Sello S, Perotto J, Carraretto L, Szabò I, Vothknecht UC, Navazio L. 2016. Dissecting stimulus-specific Ca2+ signals in amyloplasts and chloroplasts of Arabidopsis thaliana cell suspension cultures. Journal of Experimental Botany **67**, 3965–3974.
Shin S, Lee J, Rudell D, Evans K, Zhu Y. 2015. Transcript profiles of auxin efflux carrier and IAA-Amido synthetase genes suggest the role of auxin on apple (Malus domestica) fruit maturation patterns. American Journal of Plant Sciences **6**, 620–632.
Shinohara H, Mori A, Yasue N, Sumida K, Matsubayashi Y. 2016. Identification of three LRR-RKs involved in perception of root meristem growth factor in Arabidopsis.

Proceedings of the National Academy of Sciences **113**, 3897–3902.
Shinozaki Y, Hao S, Kojima M, *et al.* 2015. Ethylene suppresses tomato (Solanum lycopersicum) fruit set through modification of gibberellin metabolism. The Plant Journal **83**, 237–251.
Song W, Liu L, Wang J, *et al.* 2016. Signature motif-guided identification of receptors for peptide hormones essential for root meristem growth. Cell Research **26**, 674–685.
Stepanova AN, Yun J, Likhacheva AV, Alonso JM. 2007. Multilevel Interactions between Ethylene and Auxin in Arabidopsis Roots. The Plant Cell **19**, 2169–2185.
Tadiello A, Ziosi V, Negri AS, Noferini M, Fiori G, Busatto N, Espen L, Costa G, Trainotti L. 2016. On the role of ethylene, auxin and a GOLVEN-like peptide hormone in the regulation of peach ripening. BMC Plant Biology **16**, 44.
Tavormina P, De Coninck B, Nikonorova N, De Smet I, Cammue BPA. 2015. The Plant Peptidome: An Expanding Repertoire of Structural Features and Biological Functions. The Plant Cell **27**, 2095–2118.
Tivendale ND, Ross JJ, Cohen JD. 2014. The shifting paradigms of auxin biosynthesis. Trends in Plant Science **19**, 44–51.
Trainotti L, Tadiello A, Casadoro G. 2007. The involvement of auxin in the ripening of climacteric fruits comes of age: the hormone plays a role of its own and has an intense interplay with ethylene in ripening peaches. Journal of Experimental Botany **58**, 3299–3308.
Vancanneyt G, Schmidt R, O'Connor-Sanchez A, Willmitzer L, Rocha-Sosa M. 1990. Construction of an intron-containing marker gene: splicing of the intron in transgenic plants and its use in monitoring early events in Agrobacterium-mediated plant transformation. Molecular & general genetics: MGG **220**, 245–250.
Verwoerd TC, Dekker BM, Hoekema A. 1989. A small-scale procedure for the rapid isolation of plant RNAs. Nucleic Acids Research **17**, 2362.
Vrebalov J, Ruezinsky D, Padmanabhan V, White R, Medrano D, Drake R, Schuch W, Giovannoni J. 2002. A MADS-Box Gene Necessary for Fruit Ripening at the Tomato Ripening-Inhibitor (Rin) Locus. Science **296**, 343–346.
Wang A, Yamakake J, Kudo H, Wakasa Y, Hatsuyama Y, Igarashi M, Kasai A, Li T, Harada T. 2009. Null Mutation of the MdACS3 Gene, Coding for a Ripening-Specific 1-Aminocyclopropane-1-Carboxylate Synthase, Leads to Long Shelf Life in Apple Fruit. Plant Physiology **151**, 391–399.
Wang G, Zhang G, Wu M. 2016. CLE Peptide Signaling and Crosstalk with Phytohormones and Environmental Stimuli. Frontiers in Plant Science, 1211.
Watkins CB. 2006. The use of 1-methylcyclopropene (1-MCP) on fruits and vegetables. Biotechnology Advances **24**, 389–409.
Whitford R, Fernandez A, Tejos R, *et al.* 2012. GOLVEN Secretory Peptides Regulate Auxin Carrier Turnover during Plant Gravitropic Responses. Developmental Cell **22**, 678–685.
Zanchin A, Bonghi C, Casadoro G, Ramina A, Rascio N. 1994. Cell Enlargement and Cell Separation During Peach Fruit Development. International Journal of Plant Sciences **155**, 49–56.
Zhang S, Huang L, Yan A, Liu Y, Liu B, Yu C, Zhang A, Schiefelbein J, Gan Y. 2016. Multiple phytohormones promote root hair elongation by regulating a similar set of genes in the root epidermis in Arabidopsis. Journal of Experimental Botany **67**, 6363–6372.
Zhang Y, Yang S, Song Y, Wang J. 2014. Genome-wide characterization, expression and functional analysis of CLV3/ESR gene family in tomato. BMC Genomics **15**, 827.
Zhong S, Fei Z, Chen Y-R, *et al.* 2013. Single-base resolution methylomes of tomato fruit development reveal epigenome modifications associated with ripening. Nature

Biotechnology **31**, 154–159.

Figure Legends

Fig. 1. Expression profile of *CTG134*. (A) *CTG134* expression was barely detectable, by qRT-PCR, in non-fruit organs (small expanding leaves -sL- and fully developed leaves –LL-) and in fruit at early development (stage 1 and 2, -S1, S2-). In mature fruit (S3II) there was a sharp increase in *CTG134* transcription (S4I), slightly ceasing after the ethylene peak (S4II). (B) Ethylene, auxin and 1-MCP responsiveness of *CTG134*. *CTG134* expression, barely detectable in mature preclimacteric fruit (S3II 0) was strongly increased upon auxin (NAA, 1-naphthalene acetic acid, a synthetic auxin) but not ethylene treatment. (C) Both in Class 0 and Class 1 S4 fruit, 1-MCP upregulated *CGT134* expression. (D) Localization of *CTG134* expression in peach mesocarp by *in-situ* hybridization. In peach mesocarp at S4, *CTG134* expression was mainly associated with vascular bundles (control sections in Fig. S2). Scale bar = 50 μm.

Fig. 2. *ProCTG134:GUS* expression in tobacco and auxin responsiveness. (A, B) In tobacco roots the expression of GUS was detected at the level of the RAM (inset) but mainly at the level of lateral root primordia. (C) Staining was detectable also in leaves, especially if treated with 50μM IAA, and particularly in veins (inset). (D) In the stem, GUS expression was more abundant in parenchymatic cells of the vascular tissue. In the fruit expression was visible at the dehiscence zone (E) and in the placenta (F, G). (H) Auxin responsiveness in one-week-old representative seedlings (untreated on the left, and treaded with 50μM IAA on the right) and in the root (I, untreated, on the bottom, and treaded with 50μM IAA, on the top). Scale bar in the panels B, C and F = 500 μm, in A = 200 μm, in D = 100 μm and in E = 1000 μm.

Fig. 3. *ProCTG134:GUS* expression in *Arabidopsis*. At seven days after germination (A), GUS staining is detectable in cotyledons, especially in veins (B), at the root-shoot transition zone (D) and in lateral root primordia (E), while

is barely detectable in RAM (C). In the reproductive part, expression was detected in abscission zones before (F) and after (G) organ shedding. Expression was detectable also in maturing siliques mainly associated with vascular bundles (H). Scale bar in the panels B, C and F = 500 μm, in A = 200 μm, in D = 100 μm and in E = 1000 μm.

Fig. 4. Hormone responsiveness of *ProCTG134:GUS* in tobacco seedlings. (A) Auxin was effective in inducing the promoter of *CTG134* already at 0.5 μM, to reach almost complete saturation at 50 μM. (B) Saturation of the auxin induction after three hours. (C) Besides auxin, also 1-MCP had an inductive effect on the promoter of *CTG134*, while ethylene seemed ineffective. All experiments were carried out with T3 seedlings of line #2.

Fig. 5. Effects on root growth of *CTG134* overexpression in tobacco. (A, B) CTG134 increases hair length (ANOVA, $F = 87.75$, $df = 155$, $p < 0.001$) in tobacco plantlets grown on agar (controls are transgenic plants expressing the YFP reporter, on bottom in panel A). *CTG134* overexpression in tobacco did not saturate ethylene effect on root hair development and changed the developmental fate of epidermal cells. WT (C, E and G) and *35S:CTG134* (D, F and H) seedling roots were imaged by ESEM after growth in air (C and E) or ethylene (D and F). SEM images of the transition zones of tobacco etiolated seedling roots grown in air showed trichoblasts and atrichoblasts in the WT (G) while almost all epidermal cells were trichoblasts in *35S:CTG134* plants (H; white arrows indicate the presence of root hair primordia that are emerging from epidermal cells).

Fig. 6. Effects on root development of *CTG134* overexpression in *Arabidopsis*. CTG134 increased hair length (Measurements at 350μm from the root-stem transition zone: ANOVA, $F = 95.07$, $df = 342$, $p < 0.001$; Measurements at 1 day region after germination: ANOVA, $F = 98.31$, $df = 342$, $p < 0.001$) in *Arabidopsis* plantlets grown on agar (A and C); moreover, the portion without root hairs was reduced (ANOVA, $F = 101.1$, $df = 23$, $p < 0.001$) (A and B). Effects on root gravity perception of CTG134 in *Arabidopsis* (D) WT seedlings grown on oblique agar plates showed roots with a regular wavy patter that was altered in

CTG134 overexpressing lines (D, #3 and #23). Alteration of the wavy pattern was observed also on WT seedlings grown with synthetic CTG134 peptide added to the medium (D). The effect was stronger if the added peptide was tyrosine-sulfated (WT+SP) compared to the non-sulfated form (WT+P). Effects on root meristem size of CTG134 in *Arabidopsis* (E and F). *Arabidopsis* root sections at five DAG, stained with propidium iodide (e: WT, 35S:CTG134 = overexpressing line, WT + CTG134p = WT grown in the presence of a tyrosine-sulfated synthetic CTG134 peptide). White arrows indicate the transition zone. Scale bar = 100 μm. Measures of meristem size (F) were statistically (Tukey's multiple comparisons test) larger in comparisons among WT and overexpressing lines (#3 and #21), WT grown in the presence of a tyrosine-sulfated synthetic CTG134 peptide (WT+pCTG134) and overexpressing lines grown in the presence of a tyrosine-sulfated synthetic CTG134 peptide (#3+pCTG134 and #21+pCTG134). Meristem sizes were not statistically different if WT was excluded. Root meristem was measured using Image J software.

Fig. 7. Relative expression profiles of selected genes in roots of *Arabidopsis* seedlings grown on agar plates for five days. wt1 and wt2 are wild type samples collected from two different plates, while #3 and #21 are the clone identifiers of the *Arabidopsis* lines overexpressing the peach *CTG134* gene. Values (means of the normalized expression) have been obtained by real-time qRT-PCR analyses. Bars are the standard deviations from the means of three replicates. ACT8 was used as reference gene.

Fig. 8. Induction of a transient cytosolic Ca^{2+} change by the sulphonated peptide CTG134S in *Arabidopsis*. Cytosolic Ca^{2+} concentration ($[Ca^{2+}]_{cyt}$) was monitored in aequorin-expressing *Arabidopsis* cell cultures in response to 100 μM CTG134S (A). As controls, cells were challenged with plant cell culture medium (B) or with the non-specific peptide T16E S19A2 (100 μM, C). The arrow indicates the time of injection (100 s). Ca^{2+} traces are representative of three independent experiments which gave very similar results.

Fig. 9. A model positioning *CTG134* in the regulatory network controlling peach ripening. Regulatory data collected from the *Arabidopsis* CTG134

overexpressing clones are represented by dashed lines. Ethylene autocatalytic synthesis and action on fruit ripening is represented in blue, auxin, 1-MCP and CTG134 interactions in green, red and black, respectively. Hormones (or inhibitors) are in hexagons, their precursors in pentagons while genes (gene products) are in rectangles. Filled arrow means induction, while blunted lines repression.

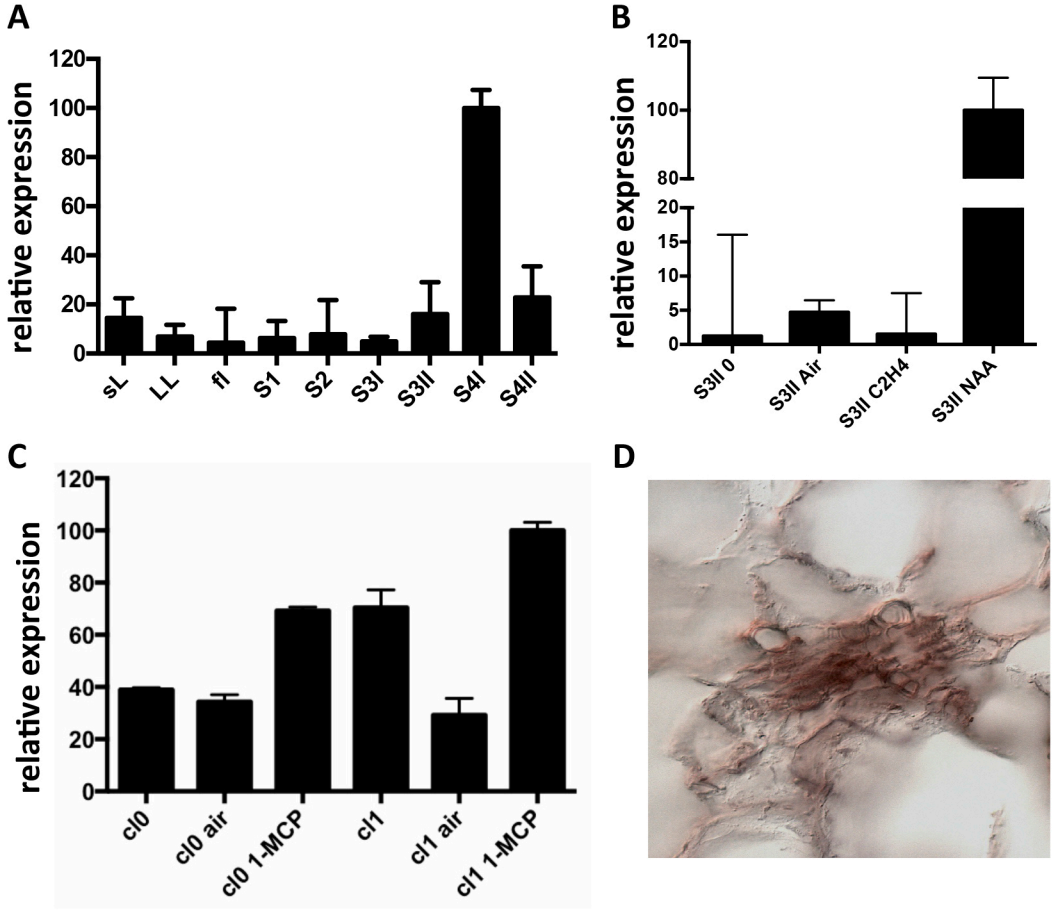
A
relative expression
120
100
80
60
40
20
0
sL
LL
fl
S1
S2
S3I
S3II
S4I
S4II
B
relative expression
120
100
80
20
15
10
5
0
S3II 0
S3II Air
S3II C2H4
S3II NAA
C
relative expression
120
100
80
60
40
20
0
cl0
cl0 air
cl0 1-MCP
cl1
cl1 air
cl1 1-MCP
D

Figure 1

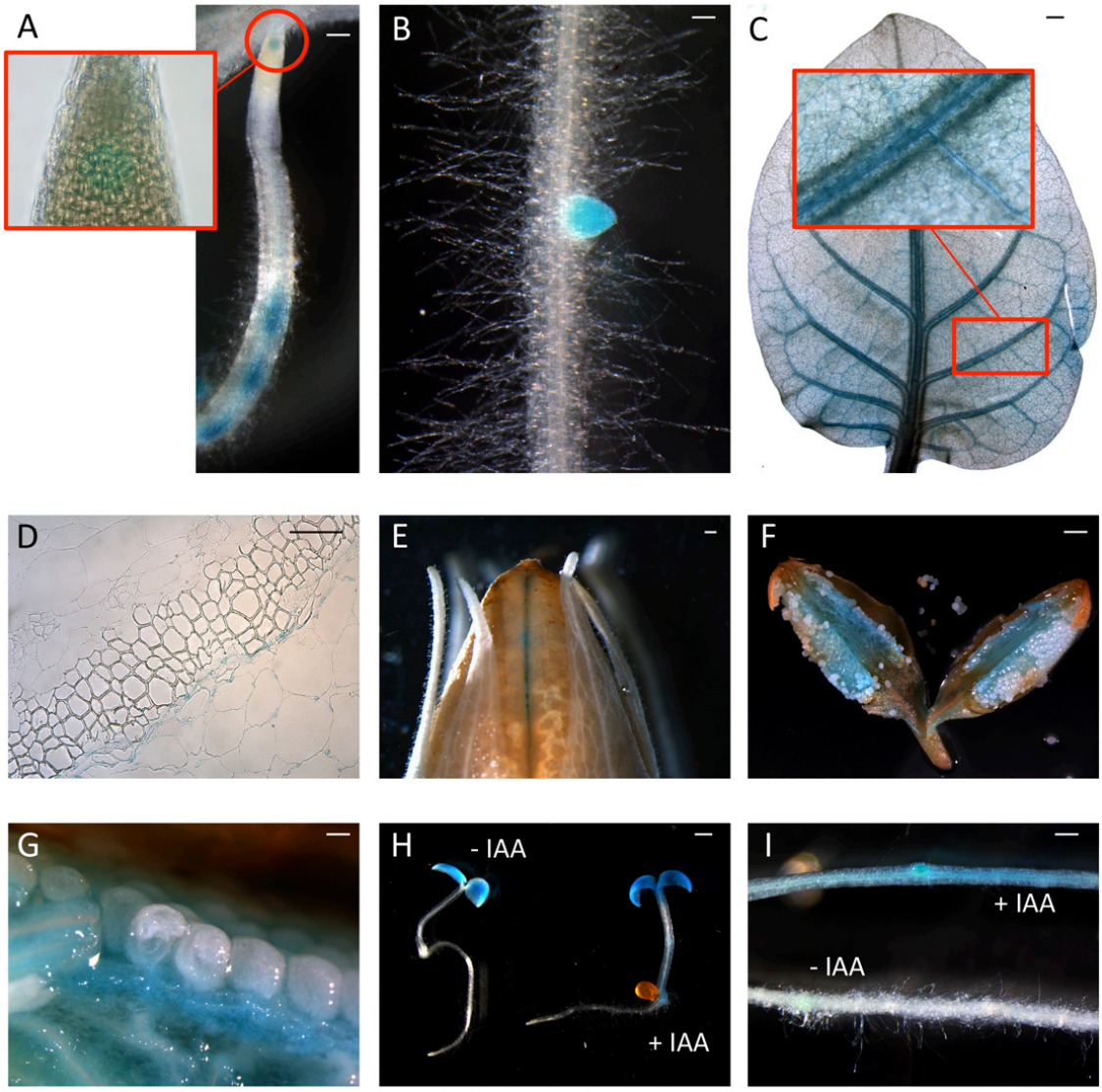

Figure 2

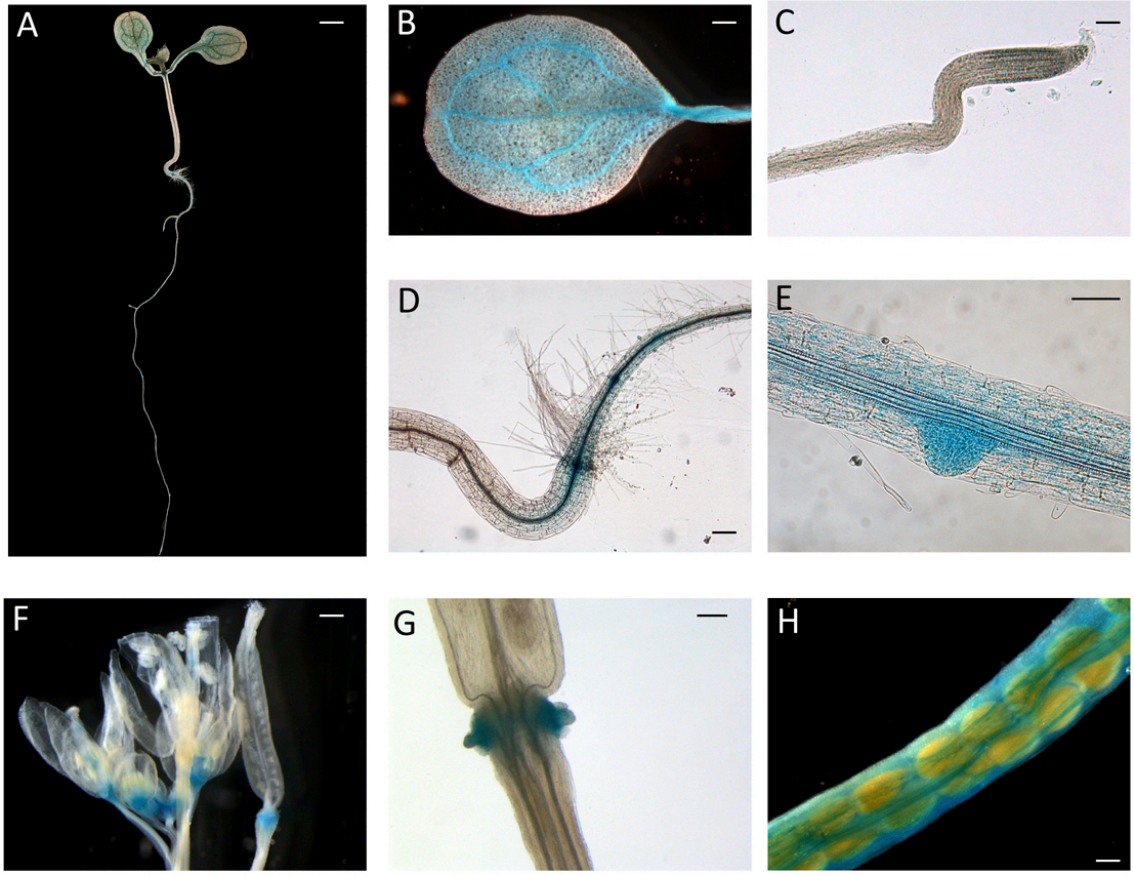

Figure 3

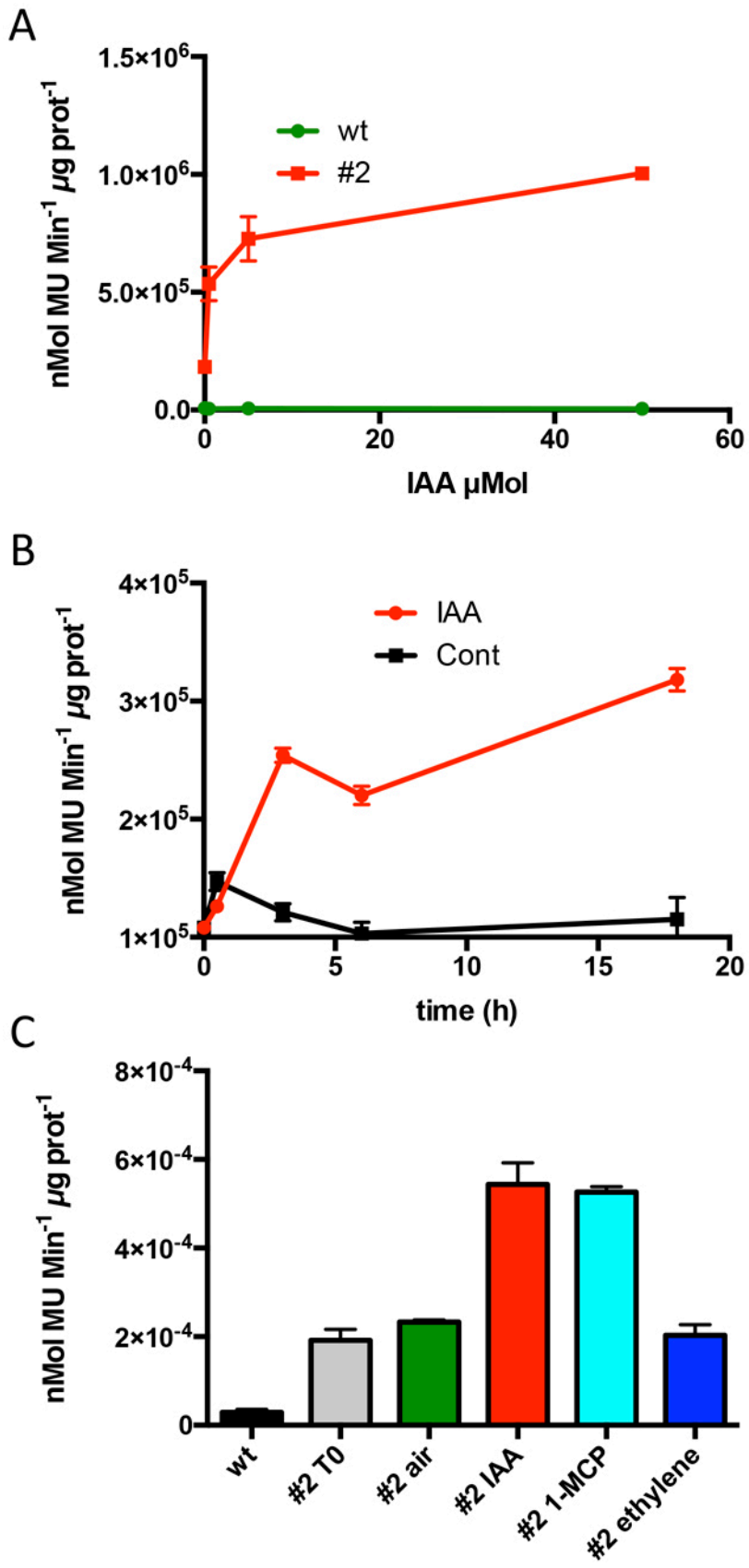
A
1.5×10^6
1.0×10^6
5.0×10^5
0.0
nMol MU Min^-1 µg prot^-1
wt
#2
0
20
40
60
IAA µMol
B
4×10^5
3×10^5
2×10^5
1×10^5
nMol MU Min^-1 µg prot^-1
IAA
Cont
0
5
10
15
20
time (h)
C
8×10^-4
6×10^-4
4×10^-4
2×10^-4
0
nMol MU Min^-1 µg prot^-1
wt
#2 T0
#2 air
#2 IAA
#2 1-MCP
#2 ethylene

Figure 4

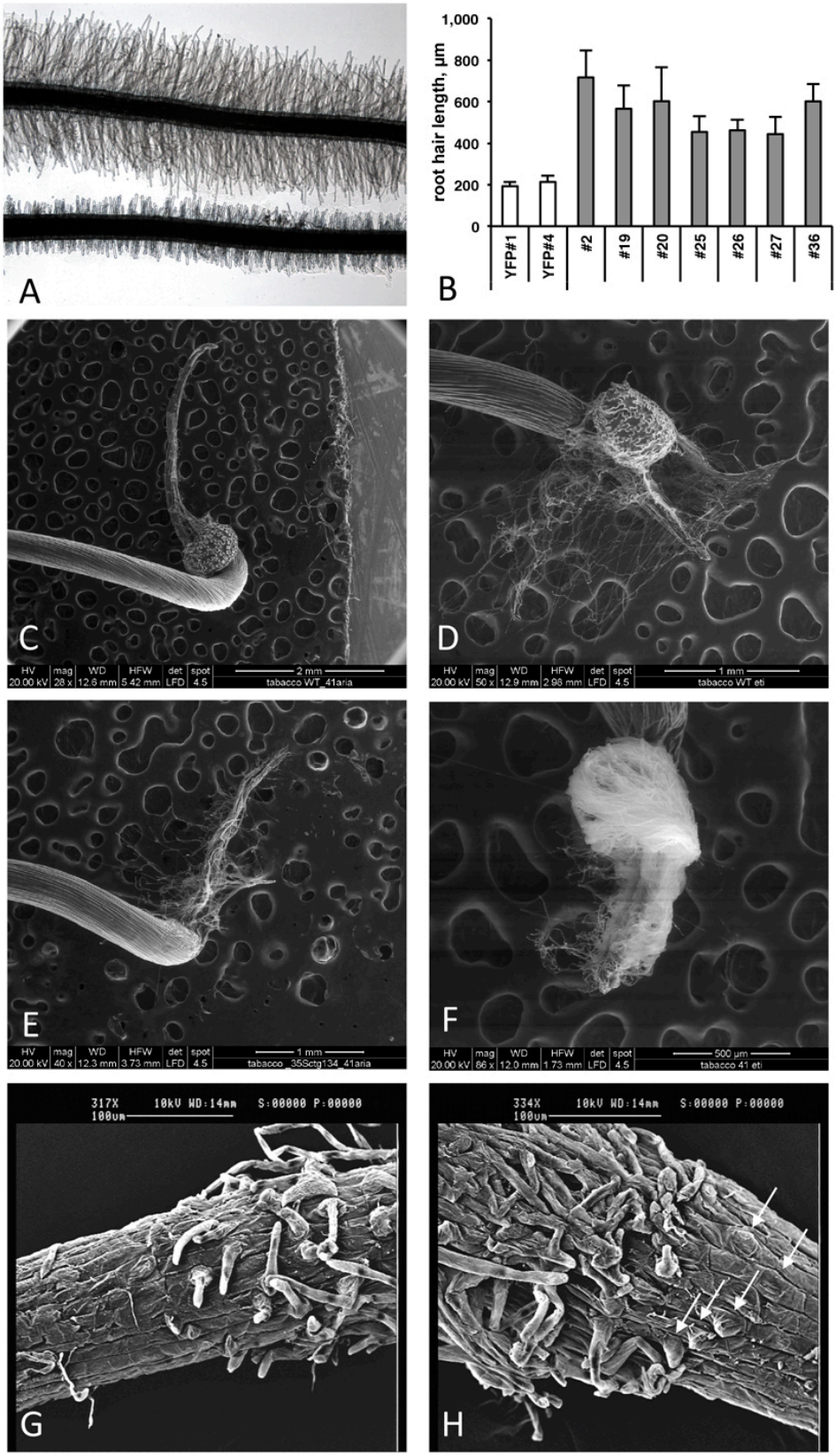
A
B
root hair length, µm
1,000
800
600
400
200
0
YFP#1
YFP#4
#2
#19
#20
#25
#26
#27
#36
C
D
E
F
G
H

Figure 5

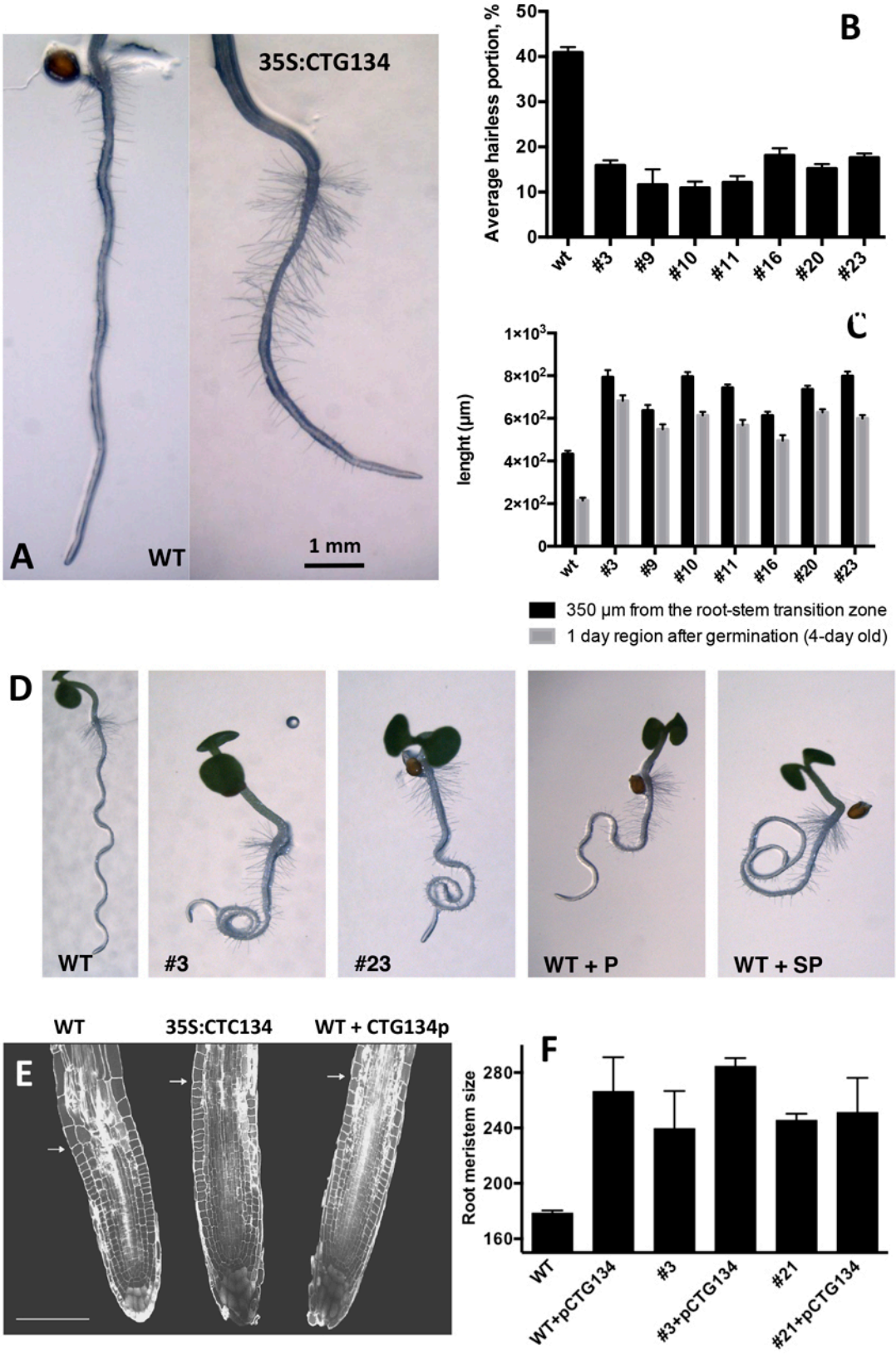
A
WT
35S:CTG134
1 mm
B
Average hairless portion, %
50
40
30
20
10
0
wt
#3
#9
#10
#11
#16
#20
#23
C
lenght (µm)
1×10³
8×10²
6×10²
4×10²
2×10²
0
350 µm from the root-stem transition zone
1 day region after germination (4-day old)
D
WT
#3
#23
WT + P
WT + SP
E
WT
35S:CTC134
WT + CTG134p
F
Root meristem size
280
240
200
160
WT
WT+pCTG134
#3
#3+pCTG134
#21
#21+pCTG134

Figure 6

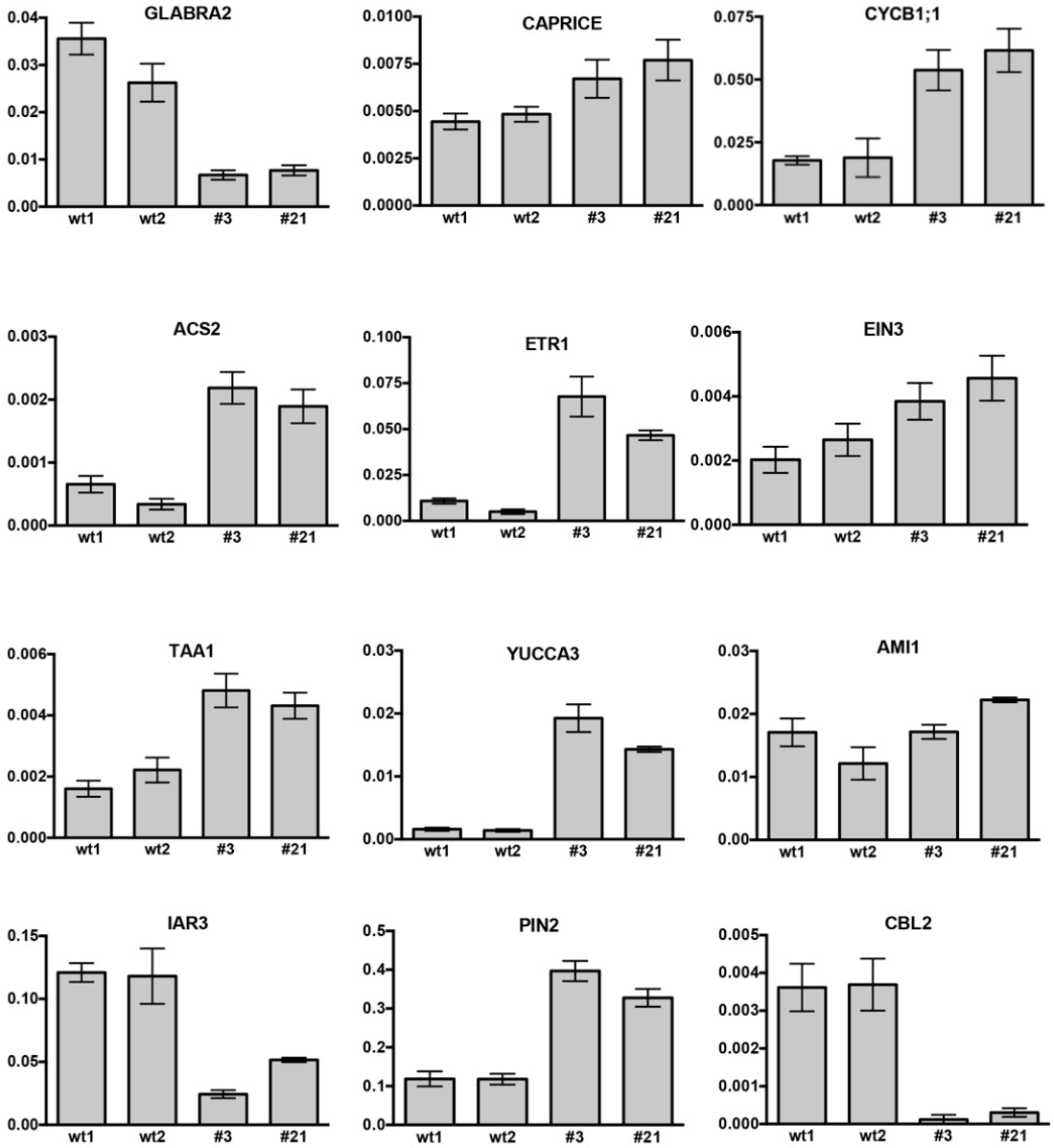
GLABRA2
0.04
0.03
0.02
0.01
0.00
wt1
wt2
#3
#21
CAPRICE
0.0100
0.0075
0.0050
0.0025
0.0000
CYCB1;1
0.075
0.050
0.025
0.000
ACS2
0.003
0.002
0.001
0.000
ETR1
0.100
0.075
0.050
0.025
0.000
EIN3
0.006
0.004
0.002
0.000
TAA1
0.006
0.004
0.002
0.000
YUCCA3
0.03
0.02
0.01
0.00
AMI1
0.03
0.02
0.01
0.00
IAR3
0.15
0.10
0.05
0.00
PIN2
0.5
0.4
0.3
0.2
0.1
0.0
CBL2
0.005
0.004
0.003
0.002
0.001
0.000

Figure 7

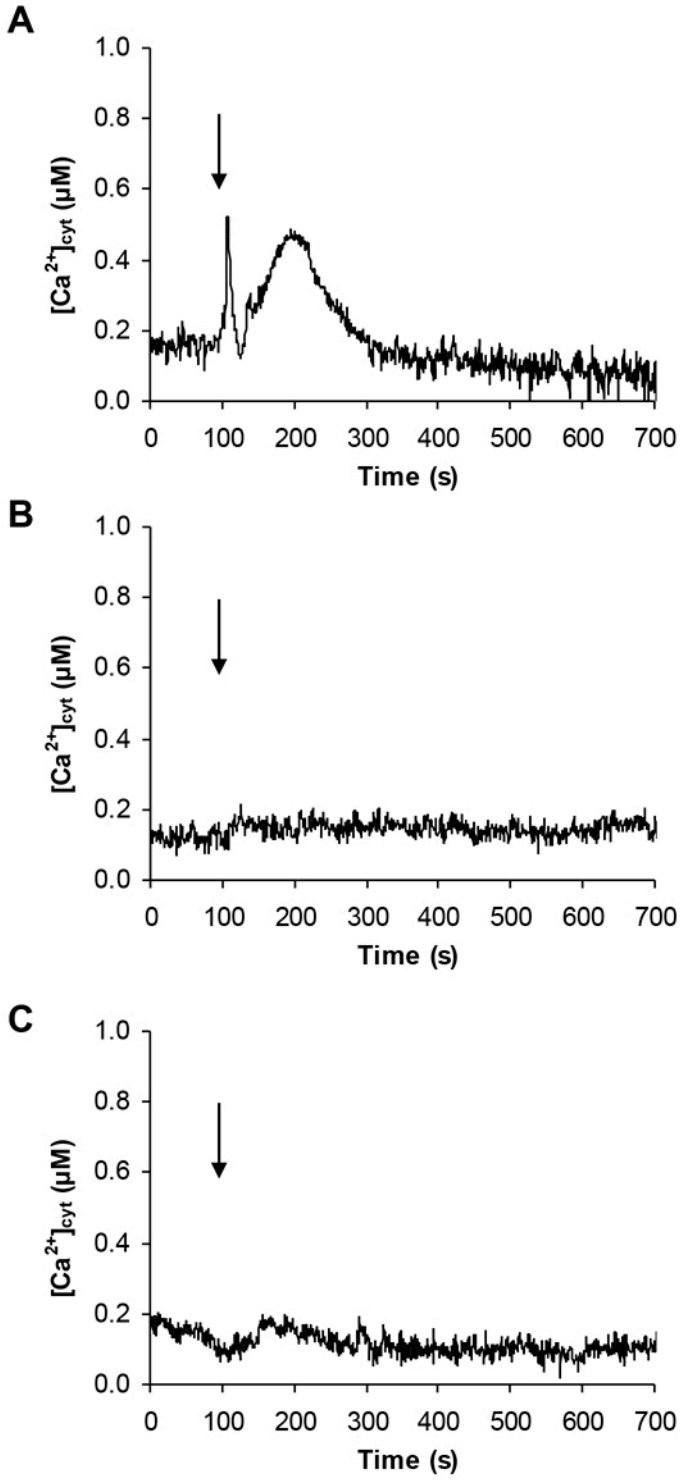
A
1.0
0.8
0.6
0.4
0.2
0.0
[Ca2+]cyt (µM)
0
100
200
300
400
500
600
700
Time (s)
B
1.0
0.8
0.6
0.4
0.2
0.0
[Ca2+]cyt (µM)
0
100
200
300
400
500
600
700
Time (s)
C
1.0
0.8
0.6
0.4
0.2
0.0
[Ca2+]cyt (µM)
0
100
200
300
400
500
600
700
Time (s)

Figure 8

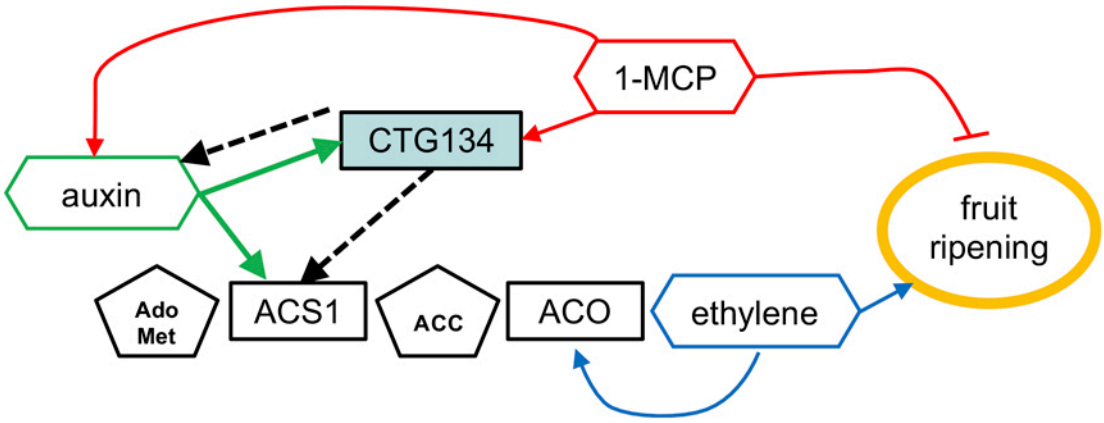
1-MCP
CTG134
auxin
fruit
ripening
Ado
Met
ACS1
ACC
ACO
ethylene

Figure 9